Available online at www.sciencedirect.com
ScienceDirect
Journal of Hazardous Materials 152 (2008) 276–286
Journal of Hazardous Materials
www.elsevier.com/locate/jhazmat

Guava (*Psidium guajava*) leaf powder: Novel adsorbent for removal of methylene blue from aqueous solutions

V. Ponnusami *, S. Vikram, S.N. Srivastava

Department of Chemical Engineering, School of Chemical & Biotechnology, SASTRA University, Thirumalaisamudram, Thanjavur 613402, India

Received 29 March 2007; received in revised form 23 June 2007; accepted 25 June 2007
Available online 5 July 2007

Abstract

Batch sorption experiments were carried out using a novel adsorbent, guava leaf powder (GLP), for the removal of methylene blue (MB) from aqueous solutions. Potential of GLP for adsorption of MB from aqueous solution was found to be excellent. Effects of process parameters pH, adsorbent dosage, concentration, particle size and temperature were studied. Temperature–concentration interaction effect on dye uptake was studied and a quadratic model was proposed to predict dye uptake in terms of concentration, time and temperature. The model conforms closely to the experimental data. The model was used to find optimum temperature and concentration that result in maximum dye uptake. Langmuir model represent the experimental data well. Maximum dye uptake was found to be 295 mg/g, indicating that GLP can be used as an excellent low-cost adsorbent. Pseudo-first-order, pseudo-second order and intraparticle diffusion models were tested. From experimental data it was found that adsorption of MB onto GLP follow pseudo second order kinetics. External diffusion and intraparticle diffusion play roles in adsorption process. Free energy of adsorption (ΔG°), enthalpy change (ΔH°) and entropy change (ΔS°) were calculated to predict the nature of adsorption. Adsorption in packed bed was also evaluated.

Keywords: Guava leaf powder; Dye removal; Batch adsorption; Fixed bed adsorption

1. Introduction

Removal of dyes from polluted effluent is an essential task for environmental protection. Considering both volume and composition, effluent from the textile industry was declared as one of the major sources of wastewater in ASEAN countries [1]. Dyes are widely used in many industries such as textile, leather, pulp & paper and plastics in order to color their products. About 700,000 tonnes and 10,000 different types of dyes and pigments are being produced annually across the world [2,3]. It is rather difficult to treat the textile wastewater by conventional biological and physical–chemical processes because of the complex molecular structure of the dyes. Therefore, innovative treatment methods are being investigated. Among the various treatment options available for the removal of dyes from textile effluents, adsorption is one of the most effective treatment methods [4]. Activated carbons are widely used as adsorbents for the removal of dyes from wastewater. However, use of activated carbon for large scale removal of dyes is quite expensive. Consequently many researchers have studied the feasibility of using low-cost substances as alternative to costly activated carbons. Materials like modified rice straw [2], fly ash [3,5], rice husk [6,7], neem leaf powder [8], chemically treated guava leaf powder [9], phoenix tree leaves [10], wheat shell [11], banana and orange peels [12], etc., have been studied. Many agro-wastes are arbitrarily discarded or set on fire generating CO_2 and other forms of air pollution. The exploitation and utilization of these materials must bring obvious economic and social benefits to mankind.

In the present work, adsorption capacity of untreated guava leaf powder (GLP) was investigated, using methylene blue as a model basic dye. Guava or *Psidium guajava* of Myrtaceae family is a tropical and semitropical plant. It is common in backyards and waste places. The raw leaves contain fixed oil 6%, and volatile oil 0.365%, resin 3.15%, tannin 8.5%, and a number of other fixed substances. Its seeds and leaves possess medicinal value and are traditionally used to treat a number of human ailments [13]. During preliminary studies carried out at our laboratory guava leaf powder had shown excellent adsorp-

* Corresponding author. Tel.: +91 99947 12632; fax: +91 4362 264120.
E-mail address: vponnu@chem.sastra.edu (V. Ponnusami).

0304-3894/$ – see front matter © 2007 Elsevier B.V. All rights reserved.
doi:10.1016/j.jhazmat.2007.06.107

Nomenclature

ARE	average relative error (ARE)
C_0	initial dye concentration in aqueous solution (mg/dm^3)
C_b	column break through dye concentration (mg/dm^3)
C_e	equilibrium dye concentration in liquid phase (mg/dm^3)
C_t	dye concentration in aqueous solution at time t (mg/dm^3)
D	adsorbent dosage (g/dm^3)
ΔG°	free energy of adsorption (J mol^{-1})
ΔH°	change in enthalpy (J mol^{-1})
I	integral constant
K_1	pseudo-first-order rate constant (min^{-1})
K_2	pseudo-second order rate constant (g mg^{-1} min^{-1})
K_a	BDST model constant (l/mg h)
K_F	Freundlich constant (mg g^{-1}) (dm^3/mg)$^{1/n}$
K_i	intraparticle diffusion rate constant (mg g^{-1} min$^{0.5}$)
K_L	Langmuir adsorption constant (dm^3 mg^{-1})
K_{Th}	Thomas model constant (l/mg h)
$LD50_{oral}$	lethal dosage 50 (oral)
m_{total}	total amount of dye sent to the column (mg)
MPSD	Marquardt's percent standard deviation
$1/n$	Freundlich parameter
N_0	The sorption capacity of the bed per unit volume of the bed (mg/l)
P	smallest level of significance leading to rejection of the null hypothesis
q_e	equilibrium dye concentration in solid phase (mg g^{-1})
$q_{eq,\,ex}$	equilibrium dye concentration in solid phase obtained from experiments (mg g^{-1})
$q_{eq,\,th}$	equilibrium dye concentration in solid phase predicted from models (mg g^{-1})
q_m	Langmuir isotherm parameter, maximum dye adsorbed/unit mass of adsorbent (mg g^{-1})
q_o	maximum dye solid phase concentration of dye in the column (mg g^{-1})
q_t	amount of dye adsorbed per unit mass of adsorbent at time t (mg g^{-1})
q_{total}	total amount of dye adsorbed in the column (mg)
Q	Column feed flow rate (ml/min)
$\%R_t$	percentage dye removed at time t (min)
R	the gas universal constant (8.314 J/mol K)
R_L	Langmuir separation or equilibrium parameter
ΔS°	change in entropy (J mol^{-1} K^{-1})
SSE	sum of the squares of error
SAE	sum of absolute errors
t	time (min)
t_b	column break through time (min)
T	absolute temperature (K)
U_0	superficial velocity of the solution (cm/h)
V_{eff}	effluent volume (ml)
x_i	process parameters (coded)
x_1	initial concentration of the dye (mg dm^{-3})
x_2	time (min)
x_3	temperature (K)
X_i	process parameters (uncoded)
Z	bed height (cm)

Greek letters

β_0	constant coefficients
β_i, β_{ii}, β_{ij}	coefficients for linear, quadratic and interaction effect
χ^2	Chi-square

tion capacity for methylene blue. The objectives of the present study were, to examine the adsorption characteristics of guava leave powder, to study the feasibility of its use as low-cost adsorbent, to determine the batch kinetic parameters, to predict the maximum possible adsorption capacity and to study the performance of packed bed adsorption. Due to its abundant availability and low-cost it can be disposed off after use without need for expensive regeneration.

Color in waterbody is aesthetically unpleasant, and interferes light penetration and reduces photosynthetic activities. Many dyes or their metabolites have toxic effects as carcinogenic, mutagenic and teratogenic effects on aquatic life and humans [2]. The methylene blue (MB, Chemical formula: $C_{16}H_{18}N_3SCl$; FW: 319.86 g/mol, λ_{max} = 662 nm, class: thiazine, C.I. Classification Number: 52015.) was chosen as a model dye because of its well known adsorption characteristics. The dye is not regarded as acutely toxic, but it can have various harmful effects. Workers handling methylene blue are at risk for photoirritant contact dermatitis (PICD) [14]. High concentration of solid dye in contact with eye has been known to have caused corneal and conjunctival injury in human beings. Hemolytic anemia has occurred in man a week after excessive doses of methylene blue. In adults IV doses in range of 500 mg have produced nausea, abdominal and precordial pain, dizziness, headache, profuse sweating and mental confusion [15]. MB is a known teratogen that results in intestinal atresia when injected intra-amniotically [16]. Methylene blue may also result in hemolytic anemia, hyperbilirubinemia, and acute renal failure [17]. $LD50_{oral}$ values for rats and mouse have been reported to be 1180 and 3500 mg/kg^{-1} [18].

2. Materials and methods

Mature guava leaves were washed thoroughly with distilled water to remove dust and other impurities and dried at 343 K in hot air oven overnight. Dried leaves were then ground, screened, washed and dried again. Dried GLP was stored in plastic containers for further use. Characteristics of the GLP were determined, and results are summarized in Table 1. The MB dye (82% dye content) was obtained from Ranbaxy Laboratories Limited

Table 1
Physical and chemical properties of GLP used in the experiments

Moisture content (%)	4.77
Volatile matter (%)	69.91
Ash (%)	19.56
Fixed carbon (%)	5.76
Bulk density (g/dm^3)	262
Average particle size, BSS #−100 + 150 (μm)	125

(India), and used without further purification. A stock solution was prepared by dissolving required amount of dye in double distilled water which was later diluted to required concentrations. All the solutions were prepared in double distilled water. Solution pH was adjusted by adding either HCl or Na_2CO_3 as required. Concentrations of the dye solutions were determined from the absorbance of the solution at the characteristic wavelength (λ_{max} = 662 nm) of MB using a double beam UV–vis spectrophotometer (Systronics 2201). Samples were diluted if the absorbance exceeds 0.8. Final concentration was then determined from the calibration curve.

Percentage dye removal was calculated using the following formula.

$$\%R_t = \frac{C_0 - C_t}{C_0} \times 100 \quad (1)$$

Specific uptake was calculated by:

$$q_t = \frac{C_0 - C_t}{D} \quad (2)$$

2.1. Adsorption experiments

The batch adsorption experiments were carried out by varying initial dye concentrations, initial pH, temperature, adsorbent dosage, and particle size. In each experiment accurately weighed GLP was added to 100 cm^3 of aqueous dye solution taken in a 250 cm^3 conical flask and the mixture was agitated at 200 rpm in an incubated shaker at a constant temperature. Samples were withdrawn at regular time intervals and centrifuged (Remi Research centrifuge). The dye concentration in supernatant solution was determined using UV–vis Spectrophotometer. All the experiments were conducted in duplicates and average values were taken.

2.2. Adsorption isotherms

Equilibrium data commonly known as adsorption isotherms are basic requirements for the design of adsorption systems. These data provide information on the capacity of the adsorbent or the amount required to remove a unit mass of pollutant under the system conditions. Langmuir and Freundlich isotherms were used to describe the equilibrium characteristics of adsorption. An accurate isotherm is important for design purposes. Linear regression is commonly used to determine the best fit model, and the method of least squares has been widely used for obtaining the isotherm constants. It is however, well known that obtaining the parameters of a non-linear equation using its linear form may introduce large errors [1]. The non-linear regression of untransformed data is therefore preferred. Non-linear regression is performed using CurveExpert 1.34 (Microsoft). Five different error functions, sum of the squares of error (SSE), sum of absolute errors (SAE), average relative error (ARE), Marquardt's percent standard deviation (MPSD), and Chi-square (χ^2) of nonlinear regressions were employed to find out the most suitable isotherm model. Definitions of these error functions are described elsewhere [1,3,19].

One of the most popular adsorption isotherms used for liquids to describe adsorption on a surface having heterogeneous energy distribution is Freundlich isotherm. It is given as:

$$q_e = K_F C_e^{1/n} \quad (3)$$

Freundlich isotherm is derived assuming heterogeneity surface. K_F and n are indicators of adsorption capacity and adsorption intensity, respectively [11]. Rearranging Eq. (3) we get,

$$\ln q_e = \ln K_F + \frac{1}{n} \ln C_e \quad (4)$$

A plot of log q_e versus log C_e yields a straight line, with a slope of $1/n$ and intercept of $\ln K_F$. The value of Freundlich constant (n) should lie in the range of 1–10 for favorable adsorption [11].

Langmuir isotherm, applicable for homogenous surface adsorption, is given as:

$$q_e = q_m \frac{K_L C_e}{1 + K_L C_e} \quad (5)$$

Eq. (5) can be rearranged into linear form:

$$\frac{1}{q_e} = \frac{1}{q_m K_L C_e} + \frac{1}{q_m} \quad (6)$$

By plotting $1/q_e$ versus $1/C_e$, the Langmuir constants can be obtained. The essential characteristics of Langmuir isotherm can be expressed by a separation or equilibrium parameter, which is a dimensionless constant defined as:

$$R_L = \frac{1}{1 + K_L C_0} \quad (7)$$

R_L indicates the nature of adsorption [11] as indicated below:

- unfavorable $R_L > 1$;
- linear $R_L = 1$;
- favorable $0 < R_L < 1$;
- irreversible $R_L = 0$.

2.3. Adsorption kinetic studies

The transient behavior of the dye sorption process was analyzed by using the pseudo-first-order, pseudo-second-order, and intraparticle diffusion models. Application of a single kinetic model to sorption on solid adsorbents may be questionable because of the heterogeneity of adsorbent surfaces and diversity of adsorption phenomena [20].

2.3.1. Pseudo-first-order model

The pseudo-first-order kinetic model has been widely used to predict dye adsorption kinetics. The pseudo-first-order rate

expression suggested originally by Lagergren based on solid capacity [8] is expressed as follows.

$$\frac{dq_t}{dt} = K_1(q_e - q_t) \quad (8)$$

Integrating and applying boundary conditions $q_t|_{t=0} = 0$ and $q_t|_{t=t} = q_t$ we get,

$$\log(q_e - q_t) = \log q_e - \frac{K_1}{2.303}t \quad (9)$$

Values of q_e and K_1 can be obtained from the slope and intercept of the plot $\log(q_e - q_t)$ versus t/2.303.

2.3.2. Pseudo-second order model

Pseudo-second order model is expressed by the equation [21].

$$\frac{dq_t}{dt} = K_2(q_e - q_t)^2 \quad (10)$$

Integrating and applying boundary conditions $q_t|_{t=0} = 0$ and $q_t|_{t=t} = q_t$ we get,

$$\frac{1}{q_e - q_t} = \frac{1}{q_e} + K_2 t \quad (11)$$

We can rearrange Eq. (11) as:

$$\frac{t}{q_t} = \frac{1}{K_2 q_e^2} + \frac{t}{q_e} \quad (12)$$

Values of q_e and K_2 can be obtained from the slope and intercept of the plot t/q_t versus t.

2.3.3. Intraparticle diffusion studies

It is necessary to identify the steps involved during adsorption in order to interpret the mechanism of adsorption. It is assumed that the adsorption process consists of several steps. Migration of the dye from the bulk of the solution to the sorbent surface, diffusion of the dye through the boundary layer, intraparticle diffusion, and adsorption of the dye on the internal sorbent surface. The intraparticle diffusion rate can be expressed in terms of the square root time. The mathematical dependence of q_t versus $t^{0.5}$ is obtained if the sorption process is considered to be influenced by diffusion in the spherical particles and convective diffusion in the solution. The root time dependence, the intraparticle diffusion model [11] is defined as follows:

$$q_t = K_i t^{0.5} + I \quad (13)$$

The plot q versus $t^{0.5}$ is given by multiple linear regions representing the external mass transfer followed by intraparticle or pore diffusion [7].

2.3.4. Thermodynamic studies

Thermodynamic parameters Gibbs free energy (ΔG°), change in enthalpy and (ΔH°) change in entropy (ΔS°) were obtained from the experiments carried out at different temperatures. The free energy of adsorption (ΔG°) can be related with Langmuir adsorption constant [3] by the following equation:

$$\Delta G^\circ = -RT \ln K_L \quad (14)$$

Therefore, enthalpy and entropy changes can be estimated from the following equation

$$\ln K_L = -\frac{\Delta G^\circ}{RT} = \frac{\Delta S^\circ}{R} - \frac{\Delta H^\circ}{RT} \quad (15)$$

Thus, a plot of $\ln K_L$ versus $1/T$ should be a straight line. ΔH° and ΔS° values were obtained from the slope and intercept of this plot, respectively.

2.4. Column experiments

Bulk removal of MB onto GLP was investigated using packed bed of BSS #−30 + 36 size GLP particles. Larger size particles were chosen to reduce excessive pressure drop and to ensure plug flow. Glass column with internal diameter 2 cm, fitted with five sampling points at 5 cm intervals, was used for the study. At the bottom of the packing 2 cm high layer of glass beads (3 mm dia.) was used to provide uniform inlet flow to the column. Dye solution was introduced into the column at desired flow rate using a peristaltic pump. Samples were collected at regular time intervals from all the sampling points.

Performance of the column operation is described by break through curves. Break through time and shape of break through curve are very important characteristics of the column for determining the operation and dynamic response of the bed. Volume of effluent processed is calculated as:

$$V_{eff} = Qt_{total} \quad (16)$$

Total amount dye adsorbed in the column for a given feed concentration and flow rate is calculated using the formula:

$$q_{total} = \frac{Q}{1000}\int_{t=0}^{t_{total}} \left(1 - \frac{C_t}{C_0}\right) dt \quad (17)$$

If the total amount of dye passed through the column is m_{total} ($=QC_0t_{total}/1000$), then percentage dye removed is calculated as:

$$\text{Total removal } \% = \left(\frac{q_{total}}{m_{total}}\right) \times 100. \quad (18)$$

2.4.1. Bed depth service time (BDST)

Bed service depth model is a simple model that assumes a linear relationship between bed height and service time of a column. The equation can be expressed as [22]:

$$t_b = \frac{N_0 Z}{C_0 U_0} - \frac{1}{K_a C_0} \ln\left(\frac{C_o}{C_b} - 1\right) \quad (19)$$

The model ignores the intraparticle mass transfer resistance and external film resistance. With these assumptions the model reasonably fits many packed bed adsorption systems well and provides information (N_0 and K_a) useful for scale up of given adsorption system.

2.4.2. Thomas models

Successful design of a column adsorption requires prediction of concentration–time profile and maximum adsorption capacity. Thomas model is one of the most general and widely used models among various models available to describe packed bed

adsorption. Thomas model assumes the following: (i) Langmuir isotherm, (ii) no axial dispersion and (iii) second order adsorption kinetics. Linear form of the model is given by the equation [22,23]:

$$\ln\left(\frac{C_o}{C}-1\right)=\frac{K_{Th}q_0X}{Q}-\frac{K_{Th}C_0}{Q}V_{eff} \quad (20)$$

K_{Th} and q_0 determined from the slope and intercept of the plot of $\ln(C_0/C-1)$ versus t at a given flow rate.

3. Results and discussion

3.1. Isotherms

Batch experiments were carried out at different dye concentrations varying from 100 to 800 mg/dm^3. Other process parameters were kept constant (temperature = 303 K, adsorbent dose = 2 g/dm^3, shaker speed = 200 rpm, and particle size = BSS #−100 + 150). Samples were taken and analyzed at regular time intervals till equilibrium was attained. Isotherm parameters and error function values determined by non-linear regression are presented in Table 2. The data fits well with both Freundlich & Langmuir isotherms yielding high R^2 values, close to 1.0. However, the values of other error functions indicate that the non-linear regression of Langmuir model provides the best fit for the experimental data. Values of error functions ARE, SAE, SSE, MPSD and χ^2 obtained by non-linear regression of Langmuir model were 10.40, 80.68, 1501.63, 14.45 and 8.42, respectively. These values are lower than the corresponding values of Freundlich isotherm model. This confirms that non-linear regression of Langmuir model fits best with the experimental data. This observation is in agreement with results reported by Ho et al. [20], who had suggested Chi-square analysis for choosing the best fitting isotherm model, rather than the use of coefficient of determination R^2. Conformation of the experimental data into Langmuir isotherm model indicates the homogeneous nature of adsorbent surface. The value of dimensionless separation parameter, R_L, was found to be in the range of 0–1, suggesting favorable adsorption process. The value of Freundlich constant, n (3.23), also suggests beneficial adsorption in the system. Langmuir constant q_m, the maximum specific uptake, was 295.04 mg/g (dosage = 2 g/dm^3, pH 7.5, size = BSS #−100 + 150, temperature = 303 K, shaker speed = 200 rpm). Previously a number of researchers have investigated several adsorbents such as modified rice straw [2], fly ash [3,5], rice husk [6,7], neem leaf [8], chemically treated guava leaves [9], wheat shells [11], banana and orange peel [12], activated carbon [24], rattan sawdust-activated carbon [25], paspalum notatum [26], cotton waste [27] for the removal of MB from aqueous solutions. Table 3 presents the comparison of adsorption capacity of GLP for MB with that of several other low-cost adsorbents and activated carbon previously reported. The comparison clearly indicates that the capacity of GLP for adsorption MB is quite high. It can be expected that GLP would have similar capacities for dyes with similar molecular weight, structure and/or ionic load. Thus, the naturally defoliated guava leaves, a low-cost natural resource, can be effectively used to remove pollutants from effluents.

Table 2
Isotherm parameters for the removal of methylene blue by GLP (T = 303 K, C_0 = 100–800 mg/dm^3, dosage = 2 g/dm^3, rpm = 200, particle size = BSS #−100 + 150)

Langmuir isotherm		Freundlich isotherm	
Parameters	Values	Parameters	Values
K_L (dm^3/mg)	0.112	K_F (mg/g) (dm^3/mg)$^{1/n}$	62.56
q_m (mg/g)	295.04	$1/n$	0.31
Separation parameter, R_L	0.01–0.08	n	3.23
Error functions	Values	Error functions	Values
ARE	10.40	ARE	17.26
SAE	80.68	SAE	82.66
SSE	1501.63	SSE	2016.61
MPSD	14.45	MPSD	36.16
χ^2	8.42	χ^2	16.99
R^2	0.99	R^2	0.999

Table 3
Comparison of adsorption capacities of various adsorbents for MB

Adsorbent	q_{max} (mg/g)
Teak wood bark	915 [27]
Activated carbon	435 [24]
Rice husk	312.26 [27]
Untreated guava leaves	295, this work
Rattan sawdust–activated carbon	294.12 [25]
Cotton waste	278 [27]
Modified rice straw	208.33 [2]
Chemically treated guava leaves	133.33 [9]
Neem leaf powder	8.76–19.61 [8]
Rice husk	40.59 [7]
Paspalum notatum	30.4–31.4 [26]
Banana peel	20.8 [12]
Orange peel	18.6 [12]
Wheat shells	16.56–21.50 [11]
Fly ash	13.42 [5]

3.2. Kinetics

Pseudo-first-order model did not fit with the experimental data well. The values of R^2 were between 0.70 and 0.85. Second order model was found to fit with the data very well. The values of q_{exp}, q_{pre}, K_1, K_2 and the corresponding linear regression coefficient R^2 values are summarized in Table 4.

Fig. 1 shows the linearized plot of second order kinetics. Plots of t/q_t versus t were perfectly linear; R^2 values were above 0.999, indicating the conformity of second order model with experimental data and the second-order nature of the adsorption process of MB onto GLP. Similar phenomena have been observed in sorption of methylene blue onto rice husk [7], and adsorption of methylene blue onto wheat shell [11]. Ho and McKay [28] revised critically the published kinetic data for many sorbent–sorbate systems and showed that, in most cases, the pseudo-second-order model is more suitable than pseudo-first-order model.

Table 4
Adsorption kinetic parameters of MB onto GLP (T = 303 K, particle size = −100 + 150 mesh, rpm = 200, dosage = 2 g/dm^3, pH 7.5)

C_0 (mg/dm^3)	$q_{eq,ex}$	First order model			Second order model			Intra particulate diffusion		
		$q_{eq,th}$	R^2	K_1	$q_{eq,th}$	R^2	K_2	I	K_i	R^2
100	48.95	3.96	0.7012	0.0206	49.13	1.0000	0.0202	21.208	5.799	1
200	98.27	17.59	0.7154	0.0185	99.38	0.9998	0.0032	52.886	5.861	0.961
500	229.37	70.80	0.7037	0.0119	234.63	0.9996	0.0006	104.002	13.606	0.976
600	251.36	121.89	0.8484	0.0096	262.40	0.9994	0.0003	78.343	16.771	0.977
800	307.27	140.16	0.8476	0.0090	318.64	0.9994	0.0002	49.938	29.146	0.972

3.3. Intraparticle diffusion

Rather than applying first and second order adsorption mechanism for the adsorption of dye molecules it is more appropriate to use intraparticle diffusion mechanism. To investigate the mechanism of adsorption process intraparticle diffusion mechanism was studied. Weber and Moris plot [3] (q versus $t^{0.5}$) was used to investigate intraparticle diffusion mechanism. Weber and Moris plot is shown in Fig. 2. In this plot, initial linear portion seen is attributed to bulk diffusion, and the second to intraparticle/pore diffusion [3]. Plateau in the plot indicates equilibrium [29]. The slope of the linear portion of the plot has been defined as a rate parameter which characterizes the rate of adsorption in the region where pore diffusion is rate limiting. The intercept of the plot signifies the extent of boundary layer effect. The larger the intercept, the greater is the boundary layer effect [11]. Deviation from the origin may be attributed to the differences between initial and final stage rates of adsorption. The values of K_i and I are given in Table 4. The value of K_i was found to increase with increasing initial concentration of the dye solution. Similar observation was reported by Mane et al. [3] for the adsorption of brilliant green onto bagasse fly ash. The value of intercept, which is a measure of bulk film thickness increases (21.2–104) with initial concentration (100–500 mg/dm^3) first, then decreases (104–49.9) at higher concentrations (500–800 mg/dm^3). Increasing trend of the intercept value with increasing concentration was earlier reported by Mane et al. [3] for the adsorption of brilliant green dye onto bagasse flyash. Mane et al. [3] reported that the value of intercept increased from 15.5 to 55.9 when the concentration of brilliant green was increased from 50 to 200 mg/dm^3. This agrees well with the present data in the same concentration range. However, beyond 500 mg/dm^3, value of intercept decreased suggesting that at higher concentrations, sorption process is controlled by intraparticle diffusion with a minor effect of the external film.

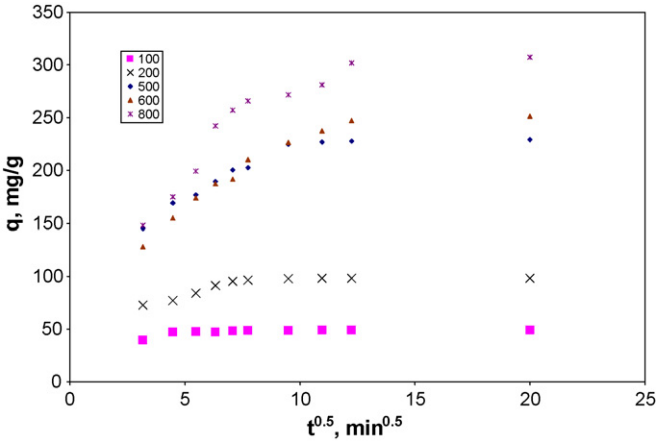

Fig. 2. Weber and Moris intraparticle diffusion plot for the removal of MB from aqueous solution. T = 303 K, rpm = 200, pH 7.5, particle size = BSS #−100 + 150, dosage = 2 g/dm^3.

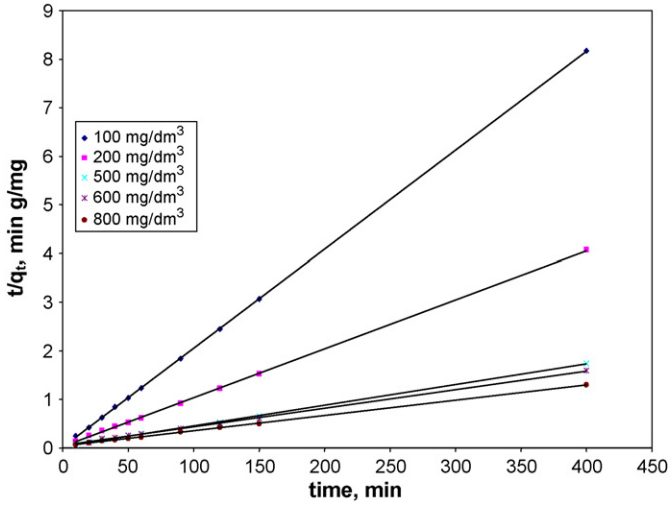

Fig. 1. Ho's second order kinetics for MB adsorption onto GLP. T = 303 K, rpm = 200, pH 7.5, particle size = BSS #−100 + 150, dosage = 2 g/dm^3.

3.4. Thermodynamic studies

ΔG°, ΔH° and ΔS° obtained from Eqs. (14) and (15) are given in Table 5. The estimated values of ΔG° for adsorption MB onto GLP were (−23.547, −24.936, 29.254 kJ/mol, respectively, at 293, 303, and 323 K which were rather low, indicating that spontaneous adsorption had occurred. Negative values of ΔG° show the feasibility and spontaneity of the adsorption process. These findings indicate a spontaneous physisorption process [11]. The enthalpy changes (ΔH°) and entropy (ΔS°)

Table 5
Values of thermodynamic parameters for the adsorption of MB onto GLP

T (K)	ΔG (J/mol)	ΔH (J/mol)	ΔS (J/mol K)	R^2
293	−23547			
303	−24936	33.200	192.966	0.9683
323	−29254			

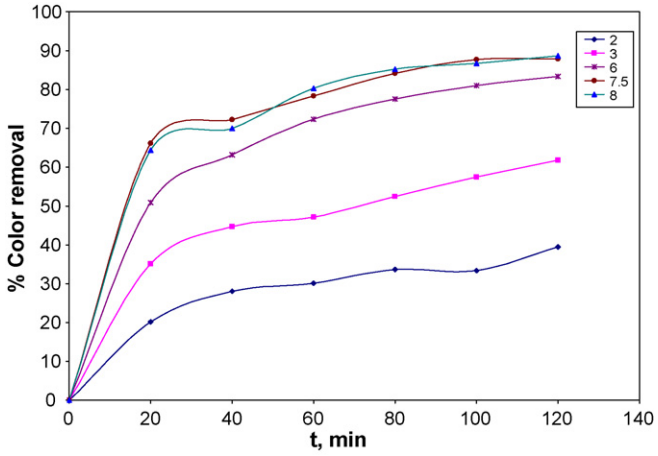

Fig. 3. Effect of pH on the removal of MB. $T = 303$ K, rpm = 200, dosage = 1 g/dm^3, particle size = BSS #−100 + 150, $C_0 = 100$ mg/dm^3.

of adsorption were 33.20 kJ/mol and $\Delta S^\circ = 192.966$ J/mol K, respectively. The positive value for ΔH° confirms that the overall adsorption of MB onto GLP is an endothermic process. The positive value of entropy change reflects the affinity of the GLP for MB and increased randomness at the solid/solution interface with some structural changes in the adsorbate and adsorbent. Also, positive ΔS° value corresponds to an increase in the degree of freedom of the adsorbed species [30].

3.5. Effect of pH

One of the important factors that affect adsorption is pH. The effect of pH on adsorption of MB onto GLP is shown in Fig. 3. It was found that the percentage color removal was less at low pH and maximum at the natural pH (7.5). At low pH (2) the maximum dye removal was 39%. Dye removal was 62, 83, 87.9, and 88.7% at pH 3, 6, 7.5 and 8 respectively. The influence of the solution pH on the dye uptake can be explained on the basis of the pH zero point charge or isoelectric point of the asorbent. The value of the pH necessary to affect a net zero charge on a solid surface in the absence of specific sorption is called the point of zero charge, pH_{pzc}. This is a convenient index of a surface when the latter becomes either positively or negatively charged as a function of pH. The pH point of zero charge (pH_{zpc}) of the adsorbent is determined by powder addition method. 0.5 g of GLP was added to 100 ml conical flask containing 50 ml of 0.1 M NaCl solution. Several batches were carried out for various initial solution pH, called pH_i. The pH was adjusted using 0.1 M HCl and 0.1 M NaOH solution. The electrolyte solution with the GLP was equilibrated for 24 h. After equilibration, the final pH, pH_f was recorded. Both positive and negative ΔpH ($pH_i - pH_f$) values recorded for the GLP are plotted against the initial pH values. The pH at which ΔpH becomes 0 is called pHpzc. The zero point charge of Guava Leaf Powder (Fig. 4) was found to be 6.25. Cation adsorption on any adsorbent will be favorable at pH > pHzpc. The surface of the adsorbent gets negatively charged and favors uptake of cationic dyes due to increased electrostatic force of attraction. Thus, MB adsorption onto GLP is favored at higher pH (value higher than 6.3). At

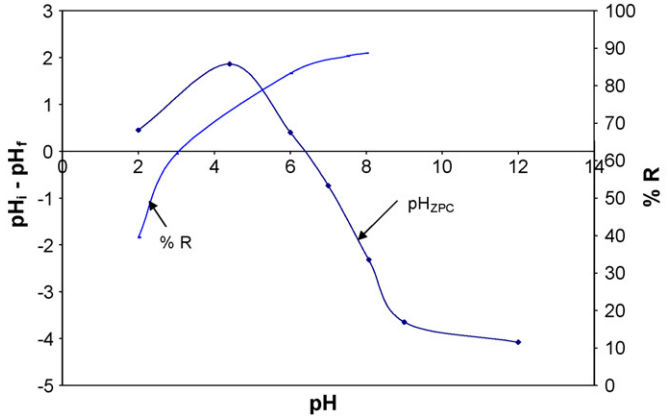

Fig. 4. Point of zero charge of GLP and effect of pH on percentage color removal.

lower pH (pH < pHzpc), adsorbent surface is positively charged, concentrations of H^+ were high and they compete with positively charged MB cations for vacant adsorption sites causing a decrease in dye uptake. Similar trend was observed for adsorption of MB onto rice husk [7], palm kernel shell activated carbon [1] and wheat shells [11]. Present results are in good agreement with the above findings. Therefore, the rest of the experiments were carried out at the natural pH of the aqueous solution.

3.6. Effect of dosage

The effect of dosage of GLP on the removal of MB was studied by varying dosage from 0.5 to 2.5 g/dm^3, keeping all other parameters constant ($C_0 = 100$ mg/dm^3, $T = 303$ K, particle size = BSS #−100 + 150, shaker speed = 200 rpm, pH 7.5). The results are shown in Fig. 5. The amount of dye removed from the aqueous solutions was 62.1, 87.9, 95.81, 97.89, and 96.19% for dosages 0.5, 1.0, 1.5, 2.0 and 2.5 g/dm^3, respectively. Since 1.5 g/dm^3 adsorbent dosage was sufficient to achieve 95.81% removal of dye from a solution of 100 mg/dm^3 further increase in dosage was not required. This can be seen from a nearly constant percentage removal obtained for higher dosages. But

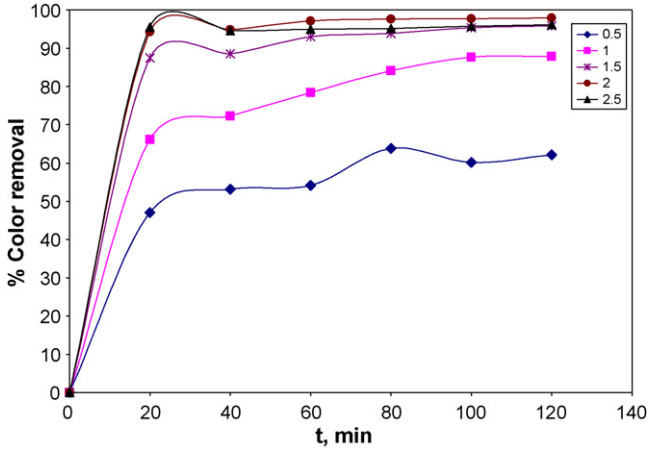

Fig. 5. Effect of adsorbent dosage for the removal of MB. $T = 303$ K, rpm = 200, pH 7.5, dosage = 0.5–2.5 g/dm^3, particle size = BSS −100 + 150, $C_0 = 100$ mg/dm^3.

at higher dosages (1.5, 2, 2.5 g/dm^3), equilibrium was attained within a short time interval (plateau is obtained in 20 min). It is obvious that an increase in adsorbent dosage increases available surface area and active sites. At a dosage of 2 g/dm^3 maximum percentage removal was obtained, under these conditions. At the same time amount of dye adsorbed per unit mass of adsorbent decreases with increase in adsorbent dosage. Uptakes were 124.2, 87.9, 63.8, 48.9, and 38.5 mg/g for dosages 0.5, 1.0, 1.5, 2.0 and 2.5 g/dm^3 respectively. This is basically due to adsorbent sites remaining unsaturated during the adsorption process.

3.7. Effect of particle size

Effect of particle size on adsorption of MB onto GLP is shown in Fig. 6. Percentage removal of dye depends much on surface area available for adsorption. Since specific surface area is more for smaller particles, it is expected that percentage removal will be more when smaller size particles are used. Dye removal was 85, 88, 95 and 94 for particle size BSS #−72 + 100, −100 + 150, −150 + 200, −200 + 250, respectively. Several investigations have shown similar observation for activated carbon and other adsorbents [6,31,32]. This relationship indicates that powdered adsorbent would be advantageous over granular particles.

3.8. Effect of temperature

Temperature is one of the most important factors that affect the adsorption rate and dye uptake. The effect of temperature on the adsorption of MB onto GLP was studied at different initial concentrations of MB. Other parameters were maintained constant (pH 7.5, dosage 1 mg/g, and particle size BSS −100 + 150). Results are presented in Fig. 7. The effect of temperature on uptake was negligible at lower concentrations (100, 200 mg/dm^3). However, at higher concentrations 400 and 600 mg/dm^3, it was observed that uptake increased first with the increasing temperature, and then decreased with further increase in temperature. Many researchers [3,6,33] have shown that adsorption increases with increase in temperature. Adsorption of *p*-nitro phenol on charred saw dust [34], biosorption of chromium onto *Sargassum* sp. [35] followed a decreasing trend of uptake with increasing temperature. In the present study it is observed that when the temperature is raised from 293 to 323 K, uptake increases initially and then decreases. A similar trend was reported for the adsorption of acid blue 29 onto a mixture of fly ash and carbon [33]. The overall adsorption process consists of several steps, bulk film diffusion, intraparticle/pore diffusion, adsorption and desorption. Adsorption capacity increases with increase in temperature if the adsorption process is endothermic and/or diffusion rate controlled. On the other hand, adsorption capacity decreases with increase in temperature if the adsorption is exothermic. Desorption in general increases with increase in temperature. Because of these varied effects of temperature on overall adsorption there should exist an optimum condition. Therefore, a search for an optimum condition was performed using statistical methods. A custom defined response surface design was used for this purpose. Initial concentration, time and temperature were the process parameters varied. Experimental range and levels of concentration, time and temperature chosen are presented in Table 6. For statistical calculations, the variables X_i were coded as x_i according to the following relationship:

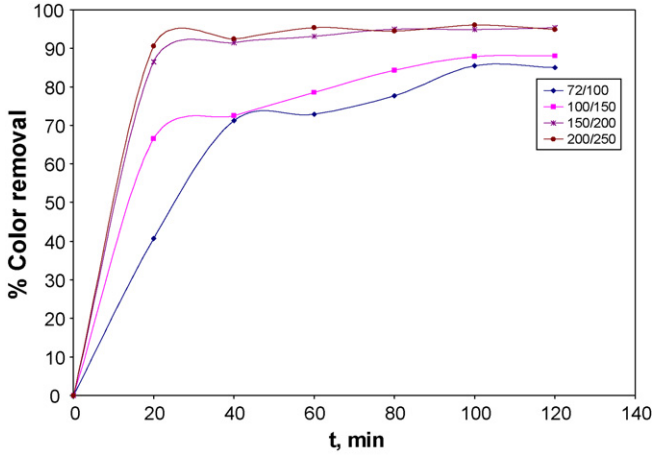

Fig. 6. Effect of particle size on the removal of MB. T = 303 K, rpm = 200, pH 7.5, dosage = 1 g/dm^3, C_0 = 100 mg/dm^3.

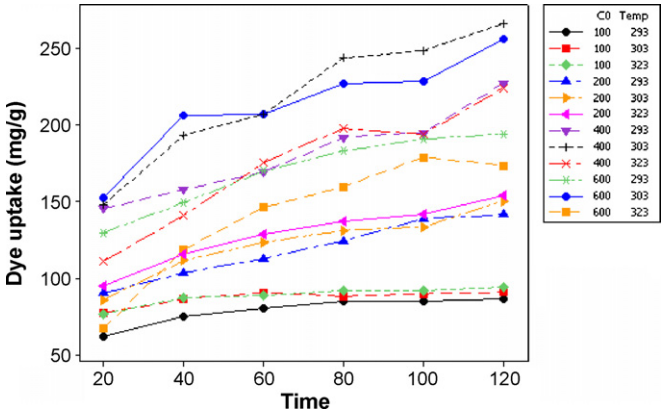

Fig. 7. Effect of temperature on the removal of MB. T = 293, 303, 323 K, pH 7.5, rpm = 200, particle size = BSS #−100 + 150, C_0 = 100, 200, 400, 600 mg/dm^3, dosage = 1 g/dm^3.

$$x_i = \left(\frac{X_i - X_o}{\delta X}\right) \quad (21)$$

A quadratic equation of the following form was used to describe the behavior of the system.

$$q_t = \beta_0 + \sum \beta_i x_i + \sum \beta_{ii} x^2 + \sum \beta_{ij} x_i x_j \quad (22)$$

The proposed model was solved using Minitab 14 (PA, USA). Model terms are statistically significant when $P < 0.05$. Esti-

Table 6
Experimental range and levels of concentration, temperature and time

Variable	Range and levels
Concentration (X_1, mg/g)	100, 200, 400, 600
Time (X_2, min)	20, 40, 60, 80, 100, 120
Temperature (X_3, K)	293, 303, 323

Table 7
Estimated regression parameters for MB uptake by GLP (in coded units)

Term	Coef	S.E. coef	T	P
Constant	202.200	5.177	39.056	0.000
C_0	46.260	2.482	18.637	0.000
Time (t)	33.665	2.789	12.071	0.000
Temp (T)	−3.335	2.333	−1.430	0.158
$C_0 \times C_0$	−49.671	4.546	−10.926	0.000
Time × time	−11.263	4.734	−2.379	0.020
Temp × temp	−27.508	4.591	−5.991	0.000
C_0 × time	17.286	3.600	4.801	0.000
C_0 × temp	−13.022	2.958	−4.402	0.000

$S = 16.03$, R-Sq = 91.8%, R-Sq(adj) = 90.8%.

mated regression coefficients and statistical parameters are listed in Table 7. The regressive model (in coded units) was obtained by substituting calculated coefficients in Eq. (22):

$$q_t = 202.2 + 46.260x_1 + 33.665x_2 - 3.335x_3 - 49.671x_1^2 - 11.263x_2^2 - 27.508x_3^2 + 17.286x_1x_2 - 13.022x_1x_3 \quad (23)$$

The data fit well with the model with reasonably high R^2 value ($R^2 = 91.8\%$ and $R^2_{\text{adj.}} = 90.8\%$). In the proposed model the term x_2x_3 was not included as the coefficient for the term x_2x_3 was not statistically significant ($P = 0.309$). Fig. 8 shows the overall trend (main effects plot) of uptake with a change in initial dye concentration and temperature. Contour plot of dye uptake by guava leaf powder is shown in Fig. 9 (corresponding to time = 120 min), indicates that the optimum temperature and concentration combination is around 500 mg/dm^3 and 303 K. The optimal values of the variables were determined by solving Eq. (23) by inverse matrix, first in coded units and then converted to uncoded units. Optimal temperature and concentration that give maximum uptake after 120 min of contact time were thus calculated to be 303 K and 517 mg/dm^3. This is in close agreement with value shown in the contour plot (Fig. 9) drawn at constant time (120 min).

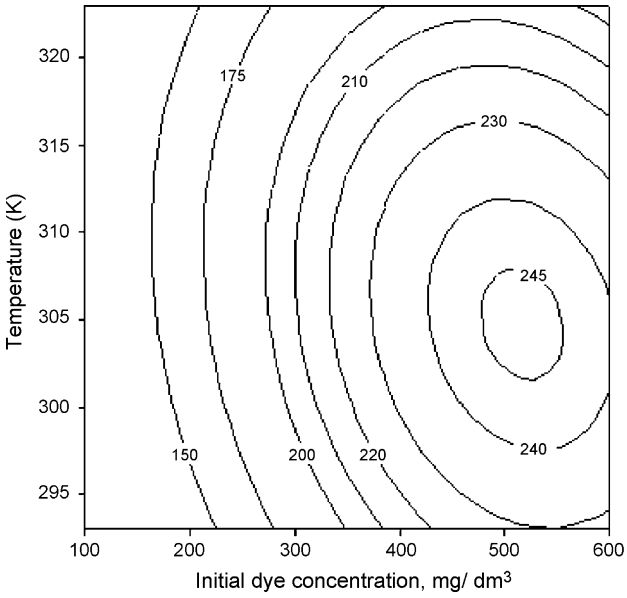

Fig. 9. Contour plot: MB uptake onto GLP vs. temperature and concentration. rpm = 200, dosage = 1 g/dm^3, particle size = BSS #−100 + 150, C_0 = 100 mg/dm^3, pH 7.5, temperature = 293–323 K.

3.9. Column studies

3.9.1. Bed depth service time

Effect of bed height was studied at constant flow rate (1.05 l/h) and initial dye concentration (200 mg/dm^3). Break through concentration was taken as $0.1C_0$ (20 mg/dm^3) and corresponding time was taken as column service time (t_b). Fig. 10 shows break through curves for MB adsorption onto GLP at different bed heights 5, 10, 15, 20 and 25 cm. Break through and exhaustion times increased with bed height as expected due to increase in the surface area of GLP available for adsorption. Plot of service time (figure not shown here) against bed height was linear ($R^2 = 99.07$). The sorption capacity of the bed per unit volume of the bed (N_0) and rate constant (K_a) were calculated from the slope and intercept of the plot, respectively. Computed N_0, and K_a were 18,290 mg/l and 0.0115 l/mg h.

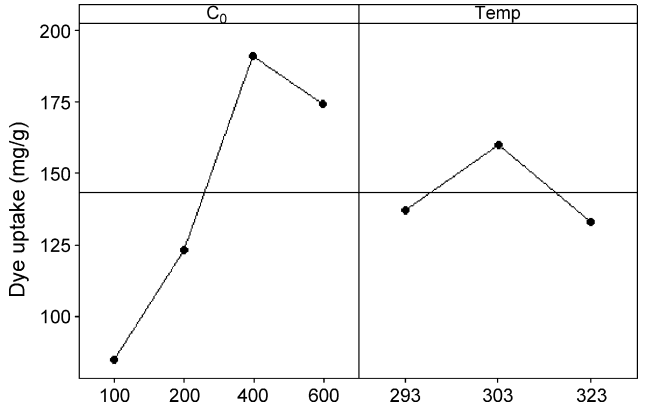

Fig. 8. Main effects plot of temperature and concentration on the removal of MB. T = 293–323 K, pH 7.5, rpm = 200, particle size = BSS #−100 + 150, C_0 = 100–600 mg/dm^3, dosage = 1 g/dm^3.

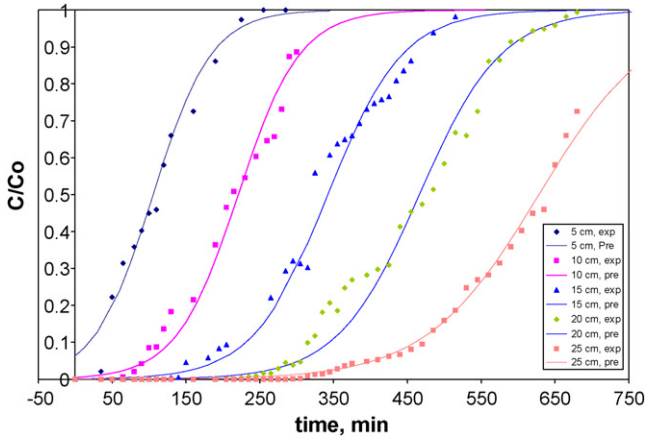

Fig. 10. Breakthrough curves for MB adsorption onto GLP at different bed heights. Flow rate = 1.05 l/h, initial dye concentration = 200 mg/dm^3, pH 7.5.

Table 8
Thomas model parameters at different heights and flow rates

Flow rate (l/h)	Bed height (cm)	q_0 (mg/g)	K_{Th} (l/mg h)	R^2
1.05	5	92.38	0.0076	95.89
1.05	10	96.63	0.0072	94.01
1.05	15	99.88	0.0059	95.10
1.05	20	102.00	0.0054	96.59
1.05	25	108.01	0.0047	93.49
0.54	5	120.71	0.0025	98.47
0.54	10	133.62	0.0023	98.35

Total dye removed calculated (assuming total service time corresponding to $C/C_0 = 0.98$) using Eq. (18) was 50.24%, 56.88%, 64.74% and 66.09% for bed heights 5, 10, 15 and 20 cm, respectively. From the break through curve shown in Fig. 10, it is evident that the length of unused bed is nearly constant. So, when the bed height is increased the ratio of length of unused bed to total height decrease. That is percentage of the bed effectively utilized increased. This results in increased percentage dye removal with increase in bed height.

3.9.2. Thomas model

Continuous adsorption of MB onto GLP packed bed was investigated. Thomas model parameters K_{Th} and q_0 determined from the slope and intercept of the plot of $\ln(C_0/C - 1)$ versus t for different flow rates and bed heights are presented in Table 8 along with corresponding coefficient of determinations (R^2). High R^2 values obtained indicate that Thomas model fit the experimental data well for this system. Comparison of experimental and predicted break through curves are shown in Figs. 10 and 11. The values of Q_0 increased and K_{Th} decreased with increase in bed height for a given flow rate. But, values of Q_0 decreased and K_{Th} increased with increasing flow rates. This is in good agreement with the observations made by Padmesh et al., [22] and Aksu and Gonen [23] for biosorption of Acid blue 15 onto *Azolla filiculoides* and phenol onto immobilized activated sludge, respectively.

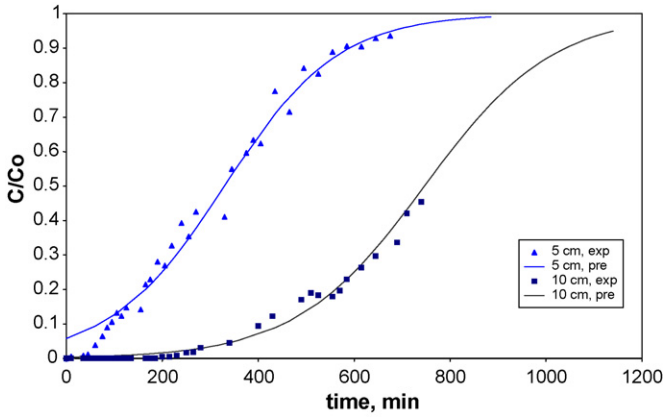

Fig. 11. Breakthrough curves for MB adsorption onto GLP at different bed heights. Flow rate = 0.54 l/h, initial dye concentration = 200 mg/dm^3, pH 7.5.

4. Conclusion

Adsorption of MB on to GLP, an agro-waste, was studied. It was shown that GLP can be used effectively for the removal of textile dyes from aqueous solutions. Batch adsorption studies were conducted to study the effects of adsorbent dosage, initial dye concentration, pH, and temperature on percentage dye removal by varying these conditions one at a time. The percentage dye removal was found to increase with increase in contact time, pH, and adsorbent dosage. With increasing initial dye concentration and temperature dye uptake increased initially and then decreased. A quadratic model was proposed to explain this behavior and the data fit reasonably well with the model proposed. Optimum temperature and concentration were 303 K and 517 mg/dm^3. The rate of adsorption was found to conform to pseudo-second-order kinetics with a good correlation coefficient. The diffusion studies confirm that more than one rate-controlling step involved in the adsorption of MB onto GLP. Equilibrium data were well explained by Langmuir isotherm. Five error functions were calculated and values of these functions were the least for non-linear regression of Langmuir model. Maximum adsorption capacity (q_m) obtained from the adsorption of MB onto GLP was 295 mg/g which was relatively high in comparison with the previous records as summarized in Table 3. The Langmuir and Freundlich isotherm parameters showed that the adsorption of MB on GLP was favorable. Thermodynamic parameters were determined. Positive ΔH° value obtained confirms that the process is physisorption. Negative ΔG° indicates feasible and spontaneous adsorption of MB onto GLP. The study confirms that GLP, an inexpensive and easily available material, can be used as an alternative for more costly adsorbents used for dye removal in wastewater treatment processes. Comparison of specific uptake of GLP for adsorption of MB, with that of other adsorbents, shown in Table 3 indicates that GLP is quite efficient for the removal of MB from aqueous solutions. It can be expected that GLP would have similar capacities for dyes with similar molecular weight, structure, and/or ionic load. Thus, the naturally defoliated guava leaves, a low-cost natural resource, can be effectively used to remove pollutants from effluents, instead of being disposed arbitrarily. Continuous adsorption of methylene blue onto GLP was investigated using a packed bed. The experimental data were well explained by Thomas model and BSDT model.

References

[1] A. Jumasiah, T.G. Chuah, J. Gimbon, T.S.Y. Choong, I. Azni, Adsorption of basic dye onto palm kernel shell activated carbon: sorption equilibrium and kinetics studies, Desalination 186 (2005) 57–64.
[2] R. Gong, Y. Jin, J. Chen, Y. Hu, J. Sun, Removal of basic dyes from aqueous solution by sorption on phosphoric acid modified rice straw, Dyes Pigments 73 (2007) 332–337.
[3] V.S. Mane, I.D. Mall, V.C. Srivastava, Use of bagasse fly ash as an adsorbent for the removal of brilliant green dye from aqueous solution, Dyes Pigments 73 (2007) 269–278.
[4] T. Robinson, G. McMullan, R. Marchant, P. Nigam, Remediation of dyes in textile effluent: a critical review on current treatment technologies with a proposed alternative, Biores. Tech. 77 (2001) 247–255.

[5] S. Wang, Y. Boyjoo, A. Choueib, A comparative study of dye removal using fly ash treated by different methods, Chemosphere 60 (2005) 1401–1407.
[6] V. Ponnusami, V. Krithika, R. Madhuram, S.N. Srivastava, Biosorption of reactive dye using acid-treated rice husk: factorial design analysis, J. Hazard. Mater. 142 (2007) 397–403.
[7] V. Vadivelan, K.V. Kumar, Equilibrium, kinetics, mechanism, and process design for the sorption of methylene blue onto rice husk, J. Coll. Interface Sci. 286 (2005) 90–100.
[8] K.G. Bhattacharyya, A. Sharma, Kinetics and thermodynamics of methylene blue adsorption on Neem (*Azadirachta indica*), Dyes Pigments 65 (2005) 51–59.
[9] D.K. Singh, B. Srivastava, Removal of basic dyes from aqueous solutions by chemically treated Psidium guyava leaves, Indian J. Environ. Health 41 (1999) 333–345.
[10] R. Han, W. Zou, W. Yu, S. Cheng, Y. Wang, J. Shi, Biosorption of methylene blue from aqueous solution by fallen phoenix tree's leaves, J. Hazard. Mater. 141 (2007) 156–162.
[11] Y. Bulut, H. Aydın, A kinetics and thermodynamics study of methylene blue adsorption on wheat shells, Desalination 194 (2006) 259–267.
[12] G. Annadurai, J. Ruey-shin, L. Duu-Jong, Use of cellulose-based waste for adsorption of dyes from aqueous solutions, J. Hazard Mater. B92 (2002) 263–274.
[13] C. Anthony, A review of Guava (*Psidium guajava*), Personal Care Mag. 6 (2005) 33–39.
[14] http://hazmap.nlm.nih.gov/cgi-bin/hazmap_generic?tbl=TblAgents&id=1026, Specialized Information Services, U.S. National Library of Medicine, 20-June-2007.
[15] http://toxnet.nlm.nih.gov/cgi-bin/sis/search/r?dbs+hsdb:@term+@rn+61-73-4, Hazardous Substances Data Bank (HSDB), U.S. National Library of Medicine (NIM), 20-06-2007.
[16] M.M. Mahadevan, G.A. Weitzman, S. Hogan, S. Breckinridge, M.M. Miller, Methylene blue but not indigo carmine is toxic to human luteal cells in vitro, Reprod. Toxicol. 7 (1993) 631–633.
[17] M. Albert, M.S. Lessin, B.F. Gilchrist, Methylene blue: dangerous dye for neonates, J. Pediatric Surg. 38 (2003) 1244–1245.
[18] http://chem.sis.nlm.nih.gov/chemidplus/jsp/common/Toxicity.jsp?calledFrom=lite, U.S. National Library of Medicine, 20-06-2007.
[19] Y.S. Ho, Selection of optimum sorption isotherm, Carbon 42 (2004) 2115–2116.
[20] Y.S. Ho, C.C. Chiang, Y.C. Hsu, Sorption kinetics for dye removal from aqueous solution using activated clay, J. Sep. Sci. Technol. 36 (2001) 2473–2488.
[21] Y.S. Ho, G. McKay, Kinetics of sorption of basic dyes from aqueous solutions by sphagnum moss-peat, Can. J. Chem. Eng. 76 (1998) 822–827.
[22] T.V.N. Padmesh, K. Vijayarhavan, G. Sekaran, M. Velan, Biosorption of Acid Blue 15 using fresh water macroalga Azollo filiculoides: batch and column studies, Dyes Pigments 71 (2006) 77–82.
[23] Z. Aksu, F. Gonen, Biosorption of phenol by immobilized activated sludge in a continuous packed: prediction of break through curves, Proc. Biochem. 39 (2004) 599–613.
[24] K. Legrouri, E. Khouya, M. Ezzine, H. Hannache, R. Denoyel, R. Pallier, R. Naslain, Production of activated carbon from a new precursor molasses by activation with sulphuric acid, J. Hazard Mater. 118 (2005) 259–263.
[25] B.H. Hameed, A.L. Ahmad, K.N.A. Latiff, Adsorption of basic dye (methylene blue) onto activated carbon prepared from rattan sawdust, Dyes Pigments 75 (2007) 143–149.
[26] K. Vasanth Kumar, K. Porkodi, Mass transfer, kinetics and equilibrium studies for the biosorption of methylene blue using Paspalum notatum, J. Hazard. Mater. 146 (2007) 214–226.
[27] G. McKay, J.F. Porter, G.R. Prasad, The removal of dye colours from aqueous solutions by adsorption on low-cost materials, Water, Air, Soil Pollut. 114 (1999) 423–438.
[28] Y.S. Ho, G. McKay, Pseudo-second order model for sorption processes, Process. Biochem. 34 (1999) 451–465.
[29] P. Janoš, P. Michálek, L. Turek, Sorption of ionic dyes onto untreated low-rank coal—oxihumolite: a kinetic study, Dyes Pigments 74 (2007) 363–370.
[30] V.C. Srivastava, B. Prasad, I.D. Mall, M. Mahadevswamy, I.M. Mishra, Adsorptive removal of phenol by bagasse fly ash and activated carbon: equilibrium, kinetics and thermodynamics, Colloid Surf. A 272 (2006) 89–104.
[31] V.K. Gupta, I. Ali, D. Suhas, Mohan, Equilibrium uptake and sorption dynamics for the removal of a basic dye (basic red) using low-cost adsorbents, J. Colloid Interface Sci. 265 (2003) 257–264.
[32] S. Wang, H. Li, Kinetic modeling and mechanism of dye adsorption on unburned carbon, Dyes Pigments 72 (2007) 308–314.
[33] K. Ravikumar, S. Krishnan, S. Ramalingam, K. Balu, Optimization of process variables by the application of response surface methodology for dye removal using a novel adsorbent, Dyes Pigments 72 (2007) 66–74.
[34] S. Dutta, J.K. Basu, R.N. Ghar, Studies on adsorption of *p*-nitrophenol on charred sawdust, Sep. Purif. Technol. 21 (2001) 227–235.
[35] M.E.R. Carmona, M.A.P. da Silva, S.G.F. Leite, Biosorption of chromium using factorial experimental design, Process. Biochem. 40 (2005) 779–788.